Available online at www.sciencedirect.com

SCIENCE DIRECT®

Journal of Molecular Catalysis A: Chemical 199 (2003) 161–174

JOURNAL OF MOLECULAR CATALYSIS A: CHEMICAL

www.elsevier.com/locate/molcata

Review

Horiuti's generalized rate expression and hydrogen electrode reaction

Hideaki Kita*

Hokkaido University, Sapporo 060-0811, Japan

Received 20 March 2002; received in revised form 10 April 2002; accepted 10 April 2002

Abstract

Horiuti's generalized rate expression is derived by using a simple model of gas effusion and then developed for heterogeneous catalysis. Characteristics of his expression are pointed out. The expression is used for estimating a rate of hydrogen evolution theoretically by taking mutual repulsive interactions among reacting species into account statistical mechanically to overcome the difficulty Tafel faced with catalytic mechanism. Results calculated on Ni(1 1 1) plane satisfactorily reproduced the experimental data observed on Ni polycrystalline electrode.

The last part reviews recent knowledge of the hydrogen evolution reaction at Pt low index planes from which we learn a new information entirely unexpected from a classical idea assuming a single kind of adsorbed hydrogen atom on the surface.

Keywords: Generalized rate expression; Rate expression of heterogeneous catalysis; Crystal plane theory; Partition function of reacting system; Adsorption isotherm with interaction; The Tafel line; Separation factor; Single crystal electrode; Upd-hydrogen; On-top hydrogen

1. Introduction

It is a great honor for the present author to submit a paper in commemoration of a centennial birthday of Professor Juro Horiuti. The author started working on the hydrogen electrode reaction under Professor Horiuti and awarded Doctor of Science in 1965, the year when Professor Horiuti retired from Hokkaido University.

Professor Horiuti devoted all his efforts to the study on the catalysis and achieved many outstanding contributions, e.g. rational explanation of linear free energy relationship based on modern concept of potential profiles [1], application of isotope to study the catalysis, i.e. tracer method [2] by using deuterium soon after its discovery, introduction of a new idea of stoichiometric number [3] offering a powerful criterion on reaction scheme, derivation of generalized rate expression [4,5] applicable to heterogeneous catalyses, especially to the reactions on crystal planes of catalyst (crystal plane theory) and so on.

He studied many representative catalyses such as ammonia synthesis, ethylene hydrogenation, acid–base catalyzed reaction but a great emphasis was placed on the hydrogen electrode reaction as a prototype of catalyses.

The present article first derives his famous generalized rate expression from a simple model of gas effusion and then develops the expression so as to be applicable for heterogeneous reactions such as catalyses reaching to the formula of potential use, especially for reactions taking place on crystal planes of catalyst.

* Tel.: +81-11-831-4535; fax: +81-11-831-4535.
E-mail address: kita@hucc.hokudai.ac.jp (H. Kita).

1381-1169/03/$ – see front matter
doi:10.1016/S1381-1169(03)00032-3

The second part treats the hydrogen electrode reaction. The most classical rate law is found by Tafel in 1905 [6], i.e. a linear relation between 'potential' (referred to the reversible hydrogen electrode) and logarithm of 'current density'. The slope (called Tafel slope) provides a key information for elucidating reaction mechanism and Horiuti succeeded in explaining rationally the value of the slope based on a so-called 'slow discharge mechanism', where the rate is controlled by the first step of proton discharge giving an adsorbed hydrogen atom. But his successive isotopic experiments led him to change his mechanism to a so-called 'recombination' or 'catalytic mechanism', where a following step of combination of adsorbed hydrogen atoms controls the reaction rate. However, a classical mass action law could not reproduce the value of the Tafel slope. Then what he noticed was mutual repulsive interactions among the species on surface. This paper represents the theoretical calculation of the reaction rate on Ni low index planes by taking the interactions into account statistical mechanically discretely.

The last section describes recent knowledges of the hydrogen electrode reaction on Pt single crystal electrode. Nowadays, single crystal electrodes of noble metals are easily available in laboratory. What have been clarified with respect to Pt single crystal electrode tell an entirely different feature of the reaction, beyond the scope of simple, classical idea of the catalysis.

2. Generalized expression of reaction rate

In 1938 [4] Horiuti derived the generalized expression for unidirectional rate, V, of any kinds of step as

$$V = \left(\frac{kT}{h}\right)\frac{QC^{\ddagger}}{QC^{\mathrm{I}}} \tag{1}$$

in terms of partition functions of $QC^{\ddagger}$ and QC^{I}. Here, a so-called transmission coefficient is equated to unity for convenience.

2.1. Derivation of Eq. (1)

Let us first define an original macroscopic assembly C as the one which includes initial systems but none of critical system, where the initial system, I, refers to a set of reacting species of a step of interest and the critical system, ‡, refers to a critical complex formed from I, respectively. Let $C^{\ddagger}$ and C^{I} be the assemblies formed from C by adding a single critical system and a single initial system from their common standard state, respectively. $QC^{\ddagger}$ and QC^{I} are the partition functions of $C^{\ddagger}$ and C^{I}.

Gas effusion is a good example to drive and understand the generalized rate expression. Let us take the macroscopic assembly C^{I} shown in Fig. 1. All the effusing molecules (mass: m, number: N) are in space A (volume: v) which is separated from a vacuum space B with a wall having a small hole (surface area: S). The effusion rate of the gas through the hole is given in textbook as

$$V = S\left(\frac{N}{v}\right)\frac{kT}{(2\pi mkT)^{1/2}} \tag{2}$$

Now, let C be an original macroscopic assembly containing $N-1$ molecules in the spaces A and B is vacuum. $C^{\ddagger}$ and C^{I} are formed from C by adding a single molecule onto the surface of the hole and into the space A, respectively. Corresponding partition functions of $QC^{\ddagger}$ and QC^{I} are given as follows.

$$\begin{aligned}
QC^{\ddagger} &= \frac{1}{(N-1)!h^{3(N-1)}}\prod_{j=1}^{N-1}\iiint \mathrm{d}x_j\,\mathrm{d}y_j\,\mathrm{d}z_j \iiint \exp\left(-\frac{p_{x_j}^2+p_{y_j}^2+p_{z_j}^2}{2mkT}\right)\mathrm{d}p_{x_j}\,\mathrm{d}p_{y_j}\,\mathrm{d}p_{z_j}\frac{1}{h^2}\\
&\quad\times\iint \mathrm{d}x_{\ddagger}\,\mathrm{d}y_{\ddagger}\iint \exp\left(-\frac{p_{x_{\ddagger}}^2+p_{y_{\ddagger}}^2}{2mkT}\right)\mathrm{d}p_{x_{\ddagger}}\\
&\quad\times\mathrm{d}p_{y_{\ddagger}} = \frac{[v(2\pi mkT)^{3/2}]^{N-1}}{(N-1)!h^{3(N-1)}}\frac{S(2\pi mkT)}{h^2}\\
QC^{\mathrm{I}} &= \frac{1}{N!h^{3N}}\int\cdots\int \exp\left(-\sum_{j=1}^{N}\frac{p_{x_j}^2+p_{y_j}^2+p_{z_j}^2}{2mkT}\right)\\
&\quad\times\prod_{j=1}^{N}\mathrm{d}x_j\,\mathrm{d}y_j\,\mathrm{d}z_j\,\mathrm{d}p_{x_j}\,\mathrm{d}p_{y_j}\,\mathrm{d}p_{z_j}\\
&= \frac{1}{N!h^{3N}}\prod_{j=1}^{N}\iiint \mathrm{d}x_j\,\mathrm{d}y_j\,\mathrm{d}z_j \iiint \exp\left(-\frac{p_{x_j}^2+p_{y_j}^2+p_{z_j}^2}{2mkT}\right)\mathrm{d}p_{x_j}\,\mathrm{d}p_{y_j}\,\mathrm{d}p_{z_j}\\
&= \frac{[v(2\pi mkT)^{3/2}]^N}{N!h^{3N}}
\end{aligned}$$

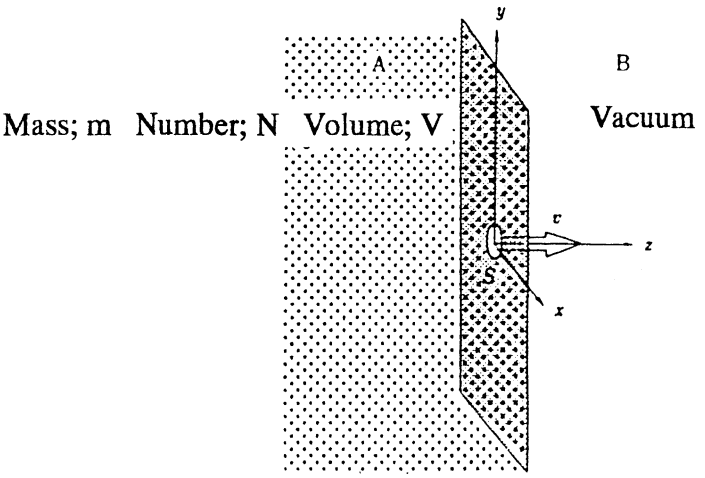

Fig. 1. Macroscopic assembly (C^{I}) for gas effusion.

where p_x, p_y and p_z are x-, y- and z-components of momentum. Thus the ratio of $QC^{\ddagger}/QC^{\mathrm{I}}$ becomes

$$\frac{QC^{\ddagger}}{QC^{\mathrm{I}}} = S\left(\frac{N}{v}\right)h\frac{2\pi mkT}{(2\pi mkT)^{3/2}} \tag{3}$$

Introducing of Eq. (3) into Eq. (2) leads to Eq. (1). Horiuti's rate expression is called 'effusion type'. Eq. (1) is general and applicable not only to physical steps but also to any chemical steps.

To be stressed in advance is that Horiuti's treatment does not insist that there is the only one critical system in reality but that a real rate is expressed by using the partition functions of the assemblies having a single critical system and none of it. In reality, there should be a number of critical systems at any moments.

Now, for a general use in chemical reactions, let us suppose a macroscopic assembly including reacting substances and others such as catalyst, electrode and, if necessary, medium like a solvent and denote it C. Related partition functions are defined as follows.

QC partition function of C

$QC^{\ddagger}$ partition function of the assembly $C^{\ddagger}$ formed from C by adding a single critical system, ‡, of a chemical step (called elementary reaction) of interest

QC^{I} partition function of the assembly C^{I} formed from C by adding a single initial system, I, of the elementary reaction

Eq. (1) is rewritten by introducing QC as

$$V = \left(\frac{kT}{h}\right)\frac{QC^{\ddagger}/QC}{QC^{\mathrm{I}}/QC} \tag{4}$$

According to a general relation between partition functions and chemical potential, μ, with respect to a species δ:

$$-RT\ln\frac{QC^{\delta}}{QC} = \mu^{\delta} \tag{5}$$

we have

$$V = \left(\frac{kT}{h}\right)\frac{QC^{\ddagger}/QC}{\exp(-\mu^{\mathrm{I}}/RT)} \tag{6a}$$

$$V = \left(\frac{kT}{h}\right)\exp\left\{-\frac{\mu^{\ddagger}-\mu^{\mathrm{I}}}{RT}\right\} \tag{6b}$$

One must notice at Eq. (6b) that Horiuti's treatment does not assume an equilibrium between the initial and critical systems. Otherwise, V becomes simply an universal constant of kT/h which is meaningless.

2.2. Application to heterogeneous reaction

Let us apply Eq. (6a) to an elementary reaction taking place on a catalyst surface. Catalyst provides the reaction with a number of reaction sites. Let us denote one of interest among them #. This # can be in various states, e.g. being vacant, occupied by ‡ or some

other adsorbates. Accordingly, we introduce the following partition functions depending on whether # is vacant or occupied by ‡.

$QC_{\#(0)}$ partition function of macroscopic assembly $C_{\#(0)}$, where # is kept vacant

$QC^{\ddagger}_{\#(\ddagger)}$ partition function of macroscopic assembly $C^{\ddagger}_{\#(\ddagger)}$ formed from C by adding a single ‡ onto the vacant #

With those partition functions, the factor $QC^{\ddagger}/QC$ in Eq. (6a) is rewritten as

$$\frac{QC^{\ddagger}}{QC} = \left(\frac{QC^{\ddagger}}{QC^{\ddagger}_{\#(\ddagger)}}\right)\left(\frac{QC^{\ddagger}_{\#(\ddagger)}}{QC_{\#(0)}}\right)\left(\frac{QC_{\#(0)}}{QC}\right) \tag{7}$$

In advance to go further, we need to comment on the surface we are concerned with. A so-called 'active center theory' assumes reaction sites having different catalytic activities each other. A total rate is given by summing up all the contributions from each site. Thus, we need to know a distribution of such sites over the surface. A so-called 'crystal plane theory', on the other hand, assumes physically equivalent reaction sites having the same catalytic activity with each other. So what we need is simply number of the reaction sites and none of their distribution with respect to catalytic activity. The crystal plane theory leads to the following physical meanings for each factor on the right-hand side of the above equation.

First factor: Since $QC^{\ddagger}$ is expressed by the sum of functions corresponding to all the possible states of # such as being vacant, occupied by ‡ or by other adsorbates, the first factor represents the reciprocal of the probability that # is occupied by ‡ added. The probability is the same all over the sites (total number: G) because of their physical equivalency and given as $1/G$. Therefore, we have

$$\frac{QC^{\ddagger}}{QC^{\ddagger}_{\#(\ddagger)}} = G \tag{8}$$

Second factor: By analogy with Eq. (5), we have

$$-RT \ln \frac{QC^{\ddagger}_{\#(\ddagger)}}{QC_{\#(0)}} = \varepsilon^{\ddagger} \tag{9}$$

where $\varepsilon^{\ddagger}$ is the reversible work required to bring ‡ from the standard state to the vacant #. Here $\varepsilon^{\ddagger}$ is not $\mu^{\ddagger}$, because ‡ is brought to the reaction site # kept previously vacant with certainty.

Third factor: A similar reasoning of the first factor is applied with respect to the macroscopic assembly C. The ratio represents a probability of # being vacant, $\theta_{\#(0)}$, i.e.

$$\frac{QC_{\#(0)}}{QC} = \theta_{\#(0)} \tag{10}$$

The value of the coverage is again common all over the sites based on the crystal plane theory.

Finally, the above three relations based on the crystal plane theory give the following formula for generalized rate expressions of Eqs. (4) and (6a):

$$V = \left(\frac{kT}{h}\right) G\theta_{\#(0)} \exp\left\{-\frac{\varepsilon^{\ddagger}}{RT}\right\} \Big/ \frac{QC^{\mathrm{I}}}{QC} \tag{11a}$$

$$V = \left(\frac{kT}{h}\right) G\theta_{\#(0)} \exp\left\{-\frac{\varepsilon^{\ddagger} - \mu^{\mathrm{I}}}{RT}\right\} \tag{11b}$$

These two equations are applied to the hydrogen evolution reaction.

3. Hydrogen electrode reaction

Hydrogen electrode reaction

$$2\mathrm{H}^{+} + 2\mathrm{e}^{-} \rightarrow \mathrm{H}_2 \tag{12}$$

is one of the most classical reactions studied from the beginning of the 20th century as a prototype of catalyses where electrodes act as catalyst.

In 1905, Tafel [6] established a relation between reaction rate (current density, i) and free energy drop ($F\eta$) as

$$\eta = a - \left(\frac{RT}{\alpha F}\right) \ln i \tag{13}$$

where η is defined as the electrode potential referred to the value of the reversible hydrogen electrode (usually called overpotential but simply potential in the text) and a and α are constants. At equilibrium ($\eta = 0$), Eq. (13) gives

$$\log i_0 = \frac{a}{2.303RT/\alpha F} \tag{14}$$

where i_0 (called exchange current density) represents an unidirectional rate at equilibrium and can be taken as a measure of the catalytic activity of the electrode used. The other constant α (called Tafel constant) gives an important information on the reaction mechanism and found as ca. 0.5 on most of metals studied. A similar value is found in the law of Brönsted and Pedersen [7] for acid–base catalyses.

3.1. Reaction mechanism of hydrogen electrode reaction

Tafel introduced an idea of the reaction scheme and rate-determining step, i.e. he assumed the hydrogen electrode reaction takes place through two steps via adsorbed hydrogen atom, H(a), as

$$H^+ + 2e^- \rightarrow H(a) \tag{15a}$$

$$H(a) + H(a) \rightarrow H_2 \tag{15b}$$

and the second step is rate-determining, i.e. the catalytic mechanism. However, he failed to explain the value of 0.5. What he obtained was 2. Namely, the initial system of the rate-determining step, 2H(a), is in equilibrium with $2H^+ + 2e^-$ through the first step and its chemical potential of μ^{I} is given as

$$\mu^{\mathrm{I}} = 2\mu(H^+) + 2\mu(e^-) = \text{constant} - 2F\eta$$

Introduction of the above relation into Eq. (11b) leads to $\alpha = 2$, provided that $\theta_{\#(0)}$ is close to unity and $\varepsilon^{\ddagger}$ remains constant independent of η.

Horiuti and Polanyi are the first persons who explained $\alpha = 0.5$ with modern concept of potential profiles assuming the first step is rate-determining, i.e. the slow discharge mechanism. This first step is taken to be a kind of acid–base catalysis satisfying the Brönsted law having an exponent of 0.5.

But shortly after the above successful explanation he needed to change his mechanism to the catalytic one. Horiuti and Okamoto [8] studied an electrolytic deuterium condensation on different metal electrodes and found an epoch-making result that the separation factor defined as

$$S_{\mathrm{D}} = \frac{i_{\mathrm{H}}/x_{\mathrm{H}}}{i_{\mathrm{D}}/x_{\mathrm{D}}}$$

differs between two groups of metals, i.e. $S_{\mathrm{D}} = 5$–6 for transition metals, whereas ca. 3 for other metals such as Hg and Pb, where i_{H} and i_{D} are the parts of current shared with H and D during the hydrogen evolution and x_{H} and x_{D} are the respective atomic fractions in the electrolyte solution. It was a well known fact that the transition metals show a good affinity toward hydrogen whereas the other metals used are not. Hirota and Horiuti [9] examined catalytic activity of transition metals for the exchange reaction of hydrogen with water and reported an activity series of metals for the reaction which is quite in harmony with that reported for a recombination of hydrogen atoms on metals by Bonhoeffer [10] (called Bonhoeffer series) as

Exchange reaction	Pt > Ni > Fe > Au > Ag ≫ Hg
Recombination	Pt > Pd > Fe > Ag > Cu

These facts strongly led him to deny the slow discharge mechanism and instead assume the catalytic mechanism for the transition metals. Thus, he had come to challenge the dilemma Tafel faced.

3.2. Catalytic mechanism

To start with, one must realize that the catalytic mechanism can take, in principle, a value from 2 to 0 for α as shown below. The factor of QC^{I}/QC of Eq. (11a) can be developed in an analogy with Eqs. (7)–(10) as

$$\frac{QC^{\mathrm{I}}}{QC} = \left(\frac{1}{\theta_{\#(0)}}\right) \exp\left(-\frac{\varepsilon^{\mathrm{I}}}{RT}\right) \theta_{\#(2\mathrm{H})} \tag{16}$$

where ε^{I} is the reversible work required to bring two hydrogen atoms from the standard state to the vacant reaction site # and $\theta_{\#(2\mathrm{H})}$ is the coverage of # being occupied with two hydrogen atoms. Introducing of Eq. (16) into Eq. (11a) gives

$$V = \left(\frac{kT}{h}\right) G \exp\left\{-\frac{\varepsilon^{\ddagger} - \varepsilon^{\mathrm{I}}}{RT}\right\} \theta_{\#(2\mathrm{H})} \tag{17}$$

The above equation tells us that when $\theta_{\#(2\mathrm{H})}$ approaches unity at high polarizations, V approaches a limiting constant value called ‘saturation current’, in other words, the slope of the Tafel relation becomes infinite and then the Tafel constant of Eq. (13) becomes zero. The value of 2 is only attainable at a limiting case where electrode surface is kept bare, i.e. $\theta_{\#(0)} = 1$.

Even so, a problem still remains that a simple mass action law expects the change of α from 2 to 0 within

a very narrow potential range of ca. 0.2 V and cannot explain a constant value of $\alpha = 0.5$ in much larger potential range as observed [11].

Then what Horiuti noticed was a mutual interactions among adsorbed species.

3.3. Mutual repulsive interactions among adsorbed species

The fact that real gas molecules exert mutual interactions encouraged him to assume the interactions among adsorbed species which are packed much more densely on the surface compared to those in gas phase. Okamoto et al. [12] introduced repulsive interactions between non-bonded surface species, i.e. between a critical system and surrounding H(a)'s as well as between H(a) of interest and surrounding H(a)'s.

3.3.1. Proportional approximation

The repulsive potentials were first taken to be proportional to a coverage of surrounding adsorption sites (denoted σ) with H(a), θ; $\varepsilon^{\ddagger}$ and $\varepsilon^{\ddagger}$ of Eq. (17) are then expressed as

$$\varepsilon^{\ddagger} = \varepsilon_0^{\ddagger} + I^{\ddagger}\theta \tag{18a}$$

$$\varepsilon^{\mathrm{I}} = \varepsilon_0^{\mathrm{I}} + I^{\mathrm{I}}\theta \tag{18b}$$

where $\varepsilon_0^{\ddagger}$ and $\varepsilon_0^{\mathrm{I}}$ are the values under the absence of the interactions and $I^{\ddagger}$ and I^{I} were taken as $K - (J/2)$, where K and J are Coulomb and exchange integrals between the atoms of interest. Horiuti [13] multiplied $I^{\ddagger}$ and I^{I} by a factor of 4.4 with reference to the adsorption heat change with coverage of hydrogen on Ni powder catalyst [14,15] and succeeded to show the Tafel constant staying almost constant $\alpha = 0.59$–0.52 in a potential range of 0.4 V.

However, the value of 4.4 is too large and furthermore the hydrogen isotherm thus obtained considerably differed from that worked out later by a higher approximation [16], where the repulsive potentials due to neighboring H(a)'s were taken into account statistical mechanically discretely based on all the possible arrangements of different number of H(a)'s at the first, second and third nearest sites (i.e. 2.49, $2.49\sqrt{2}$ and $2.49\sqrt{3}$ Å) to the H(a) of interest on Ni(1 1 0) by Bethe–Peierl's method [17,18].

3.3.2. Statistical mechanical treatment

Let us call the first, second and third approximation according as the only first, up to second and up to third nearest sites were taken into account statistical mechanically discretely. The results show that the second approximation is regarded close enough to the third one. Enhancement of approximation brings a tremendous increase of labor to calculate the isotherm theoretically. Horiuti and Toya [19] applied the second approximation to calculate the theoretical isotherm with an adjusting parameter γ on Ni(1 1 0). They found that a value of $\gamma = 1.5$ gives the best agreement with experimental ones reported on Ni powder catalyst.

Since Ni(1 1 0) plane is least dense, whereas Ni(1 1 1) is most dense among the low index planes of fcc crystal, Ni(1 1 0) plane will exert the weakest repulsive interaction and then cause hydrogen adsorption preferentially, while Ni(1 1 1) plane will be least favorable for the adsorption. Such a difference is undoubtedly expected to affect the rate of the hydrogen evolution.

4. Theoretical rate of hydrogen evolution on Ni low index planes

Then, Horiuti and Kita [11] calculated not only the hydrogen isotherm but also the rate of hydrogen evolution reaction on all the low index planes of Ni by treating the interaction statistical mechanically.

To minimize a tremendous increase of labor on the rate calculation, we used a 'combined approximation' which was confirmed accurate enough to reproduce the isotherm calculated by the second approximation on Ni(1 1 0) [20]. The combined approximation treats the repulsion exerted by the first nearest neighbors statistical mechanically discretely and those of the second and third ones by the proportional approximation. This approximation allows us to calculate the reaction rates as a function of η on all the low index planes of Ni(1 1 0), (1 0 0) and (1 1 1) for different values of $\gamma = 1.2$, 1.5 and 2.5, though the number of nearest neighbors to ‡ increases from 4 on (1 1 0) to 6 and 8 on (1 0 0) and (1 1 1), respectively. The way of counting interaction by the combined approximation is illustrated below for the (1 1 1) plane.

Combined approximation: First of all, we must remember that the catalytic mechanism requires a reaction site consisting of a pair of adjacent nearest adsorption sites of hydrogen. The initial system of 2H(a)'s also sits on #.

Let us pick up 10 adsorption sites, from σ_1 to σ_{10} (denoted Γ) as shown in Fig. 2a, where σ_1 and σ_2 forms # and the other σ's are first nearest to ‡.

The partition function of the assembly $C^{\ddagger}_{\#(\ddagger)}$ formed from $C_{\#(0)}$ by adding a single ‡ from the standard state onto the vacant # is expressed as

$$QC^{\ddagger}_{\#(\ddagger)} = \sum_{g} QC^{\ddagger}_{\Gamma\{\ddagger,g\mathrm{H}\}} = \sum_{g}\sum_{k} QC^{\ddagger}_{\Gamma\{\ddagger,k(g\mathrm{H},8\sigma)\}} \tag{19}$$

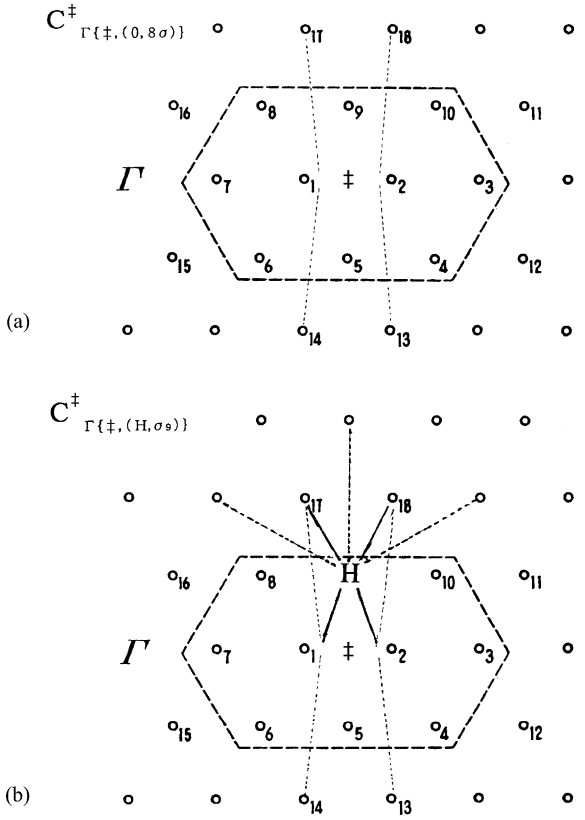

Fig. 2. Γ consists of a group of σ's selected to allow counting the first nearest interactions statistical mechanically under the presence of ‡ on σ_1 and σ_2 with (a) none of H(a)'s on σ_3–σ_{10} and (b) H(a) at σ_9. Dotted lines represent the third nearest interactions by the proportional approximation.

where the suffix $\Gamma\{\ddagger, g\mathrm{H}\}$ refers to the state of Γ that # is occupied by ‡ and the rest of eight σ's in Γ are occupied by g hydrogen atoms. $\Gamma\{\ddagger, k(g\mathrm{H}, 8\sigma)\}$ specifies further that gH(a)'s are in kth arrangements. The first $\sum$ refers to g which runs from 0 to 8 and second one refers to k which runs from 1 to $8!/g!(8-g)!$. Two examples of counting the interactions are demonstrated below.

First example, $g = 0$: We have the only ‡ at # and the other eight σ's in Γ are vacant (Fig. 2a). Corresponding partition function is obtained from that of the assembly including none of ‡, $QC_{\Gamma\{0\}}$, in analogy with Eq. (9) as

$$QC^{\ddagger}_{\Gamma\{\ddagger,(0\mathrm{H},8\sigma)\}} = QC_{\Gamma\{0\}} \exp\left(-\frac{\varepsilon^{\ddagger}}{RT}\right) \tag{20}$$

where $\varepsilon^{\ddagger}$ is the reversible work required to bring ‡ from the standard state to # of $\Gamma(0)$ and is expressed as

$$\varepsilon^{\ddagger} = \varepsilon^{\ddagger}_{0} + \gamma \mathrm{III}^{\ddagger}\theta$$

where $\varepsilon^{\ddagger}_{0}$ is the value under the absence of the interactions and $\gamma\mathrm{III}^{\ddagger}\theta$ is the interaction between the critical system and H(a)'s at the third nearest sites outside Γ (σ_{13}, σ_{14}, σ_{17} and σ_{18} in Fig. 2a), which is taken by the proportional approximation with a parameter γ. In the case of the (1 1 1) plane we do not have any second nearest sites ($2.49\sqrt{2}$ Å).

Second example, $g = 1$: We have eight arrangements depending on what site out of eight σ's is occupied by H(a). For example, when σ_9 is occupied (Fig. 2b), the corresponding partition function is derived from the above $QC^{\ddagger}_{\Gamma\{\ddagger,(0\mathrm{H},8\sigma)\}}$ by two processes: (1) one of H(a)'s outside Γ is taken out to the standard state; and (2) brought back to σ_9 of Γ. The first process introduces a factor of $\exp(\mu^{\mathrm{H}}/RT)$ to Eq. (20) by analogy with Eq. (5) and the second process introduces a factor of $\exp(-\varepsilon^{\mathrm{H}}/RT)$ to Eq. (20) by analogy with Eq. (9), where ε^{H} is the reversible work required to bring H(a) from the standard state to σ_9 under the presence of ‡. Thus, we obtain the following expression.

$$QC^{\ddagger}_{\Gamma\{\ddagger,(\mathrm{H},\sigma_9)\}} = QC_{\Gamma(0)} \exp\left(\frac{\mu^{\mathrm{H}}}{RT}\right) \exp\left\{-\frac{\varepsilon^{\ddagger} + \varepsilon^{\mathrm{H}}}{RT}\right\}$$

The reversible work ε^{H} is expressed by taking into account the interactions due to the first nearest neighbors discretely and the others by the proportional approximation as

$$\varepsilon^{\mathrm{H}} = \varepsilon_0^{\mathrm{H}} + \gamma I^{\ddagger} + 2\gamma I' + 3\gamma \mathrm{III}'\theta \quad (21)$$

where $\varepsilon_0^{\mathrm{H}}$ is the value under the absence of interactions, $\gamma I^{\ddagger}$ the interaction with ‡ at # inside Γ, $2\gamma I'$ the interaction with two first nearest H(a)'s outside Γ (namely, those on σ_{17} and σ_{18} in Fig. 2a), and $3\gamma \mathrm{III}'\theta$ is due to H(a)'s sitting on the third nearest sites outside Γ, respectively. Eq. (21) clearly shows that the interactions due to the first neighbors are taken discretely and the third ones are by the proportional approximation.

It must be noted here that whether the first nearest sites outside Γ, i.e. σ_{17} and σ_{18}, are occupied or not is unknown. Therefore, $2\gamma I'$ is treated as unknown and will be solved beforehand by other conditions as shown later. Similar treatments for the other seven possible arrangements allow us to obtain the partition function of the assembly with $\Gamma\{\ddagger, (\mathrm{H}, 8\sigma)\}$. Formulation of $QC^{\ddagger}_{\#(\ddagger)}$ is achieved by summing up all the partition functions worked out by changing g from 0 to 8 and k from 1 to $8!/g!(8-g)!$.

Similar procedures apply to QC, i.e.

$$QC = \sum_g \sum_k QC_{\Gamma\{k(g\mathrm{H}, 10\sigma)\}}$$

where g runs from 0 to 10 and k runs from 1 to $10!/g!(10-g)!$, respectively.

Thus, we can calculate the reaction rate as a function of η on the respective crystal planes by Eq. (6a), provided that θ and I' are known as a function of η at a given value of γ.

Unknowns: To determine I' and θ as a function of η in advance, the following two conditions are used:

(1) equivalency of σ's, for example, $QC_{\sigma_9(\mathrm{H})} = QC_{\sigma_8(\mathrm{H})} = QC_{\sigma_1(\mathrm{H})}$;
(2) isotherm, for example, on σ_9, $QC_{\sigma_9(\mathrm{H})}/QC_{\sigma_9(0)} = \theta/(1-\theta)$;

where each partition function is formulated with respect to Γ under conditions specified with respective suffixes. In calculation, $\varepsilon_0^{\mathrm{H}}$ on Ni(1 1 0) plane was taken as 12.3 kcal mol^{-1} from the heat of adsorption on Ni powder catalyst [14,15].

4.1. Calculated hydrogen isotherm on Ni low index planes

Fig. 3a shows the hydrogen isotherms calculated as a function of η on the low index planes at $\gamma = 1.5$. This figure shows that hydrogen adsorbs preferentially on the (1 1 0) plane on account of the smallest repulsive interaction and reaches to a full coverage around $\eta = 0$, whereas it adsorbs at more negative potentials on the other two planes and reaches to only a half on the (1 0 0) and one third on the (1 1 1) planes at $\eta = 0$, respectively.

A full coverage is achieved at ca. −0.9 V on the most dense plane of (1 1 1). Isotherm calculated by the proportional approximation on the (1 1 0) plane for comparison [11] shows a smooth increase of θ in almost the same potential range up to −0.9 V at $\gamma = 4.4$ which is too large as stated earlier.

Secondly, it is interesting to see a step wise increase of coverage on all the planes studied; two steps on the (1 1 0) and (1 0 0) planes and three steps on the (1 1 1) planes, respectively. Fig. 3b explains the way of adsorption under the presence of repulsion. Hydrogen atoms first occupy the sites, say those of solid circles, so as to minimize their mutual repulsions. When these sites are completely covered, the coverage becomes a half on the (1 1 0) and (1 0 0) planes and one third on the (1 1 1) plane. Hydrogen atoms need some more extra potential to adsorb further at open circles because of a larger repulsion from the preadsorbed H(a)'s, giving rise to a plateau on the isotherm. Sites expressed by dots on the (1 1 1) plane will give another plateau by the same reason.

4.2. Theoretical rate of hydrogen evolution on Ni low index planes

Fig. 4 shows η versus $\log i$ plot calculated on the respective planes at $\gamma = 1.5$ which gave the best fit to the experimental ones [21] observed on Ni polycrystalline wire electrode in alkaline solution. Results are commented as follows.

(1) The saturation current, characteristic of the catalytic mechanism, increases with the order of the (1 1 0), (1 0 0) and (1 1 1) planes. The current on the (1 1 0) plane under the absence of the interaction ($\gamma = 0$) shows a simple, sharp rise to

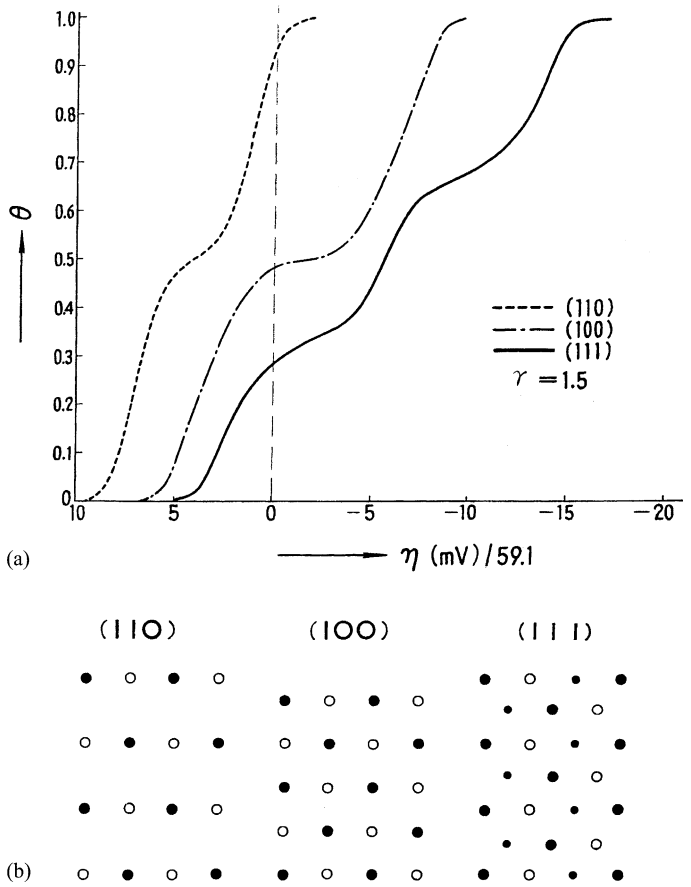

Fig. 3. (a) Theoretical isotherms of hydrogen adsorption on Ni(1 1 0), (1 0 0) and (1 1 1) planes calculated by the combined approximation for mutual repulsive interactions; γ is an adjusting parameter. (b) Two step adsorption on the (1 1 0) and (1 0 0) planes and three step adsorption on the (1 1 1) plane.

the limiting value of the saturation which is the smallest one.

(2) The (1 1 1) plane exhibits the most predominant contribution and is only the plane which reproduces the experimental data satisfactorily in a potential range of -0.2 to -0.7 V with $\gamma = 1.5$. The value of $\gamma = 1.5$ is the one concluded at the analysis of the hydrogen isotherm on Ni by the second approximation [19].

To be stressed is that the contributions from the other two low index planes are almost negligible, smaller by more than several orders of magnitude. Such an exclusive contribution of the (1 1 1) plane will be understood in terms of the repulsive interactions as follows.

In general, any repulsive interactions from surroundings give rise to an increase in a potential energy of the species of interest. In the present case, we have either the initial or critical system at the reaction site, #. The question is which one of those systems receives stronger repulsive interactions from the surroundings. When the initial system receives stronger interactions, an activation energy will become smaller, resulting in an increase of reaction rate, while the other case brings a decrease of reaction rate, respectively.

As can be figured out from Fig. 2, the initial system of a pair of adjacent H(a)'s on σ_1 and σ_2 receives stronger repulsions from the H(a)'s on σ_3–σ_{10} than the critical system on σ_1 and σ_2 does,

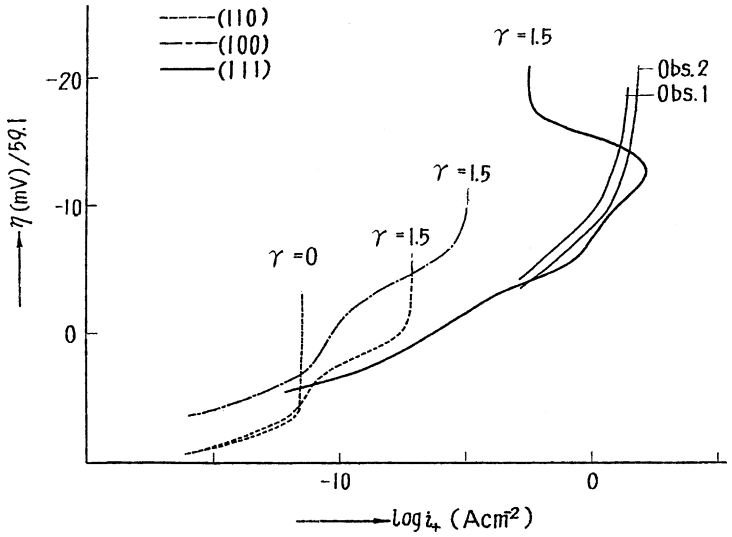

Fig. 4. Theoretical η vs. $\log i$ plots on Ni(1 1 0), (1 0 0) and (1 1 1) planes calculated by the combined approximation with $\gamma = 1.5$. For comparison, theoretical result on the (1 1 0) plane under the absence of interaction ($\gamma = 0$) is quoted. Obs. 1 and 2 represent experimental ones [21] observed on Ni polycrysalline electrode in 0.95 and 4.73 M NaOH solutions, respectively.

since the constituent two hydrogen atoms of the critical system locate more or less away from the surrounding H(a)'s in comparison to those of the initial system, as seen from a configuration of the critical system [11].

(3) A calculated η versus $\log i$ relation on the (1 1 1) plane is quite different from the others at high polarizations, where the current starts decreasing with η and finally reaches to a saturation current. This behavior is attributed to unique locations of σ_5 and σ_9 toward the critical system (Fig. 2). These sites tend to be left vacant till the other sites in Γ are occupied because of its closest position to the both of constituent H atoms of the critical system. Once these sites are occupied at high polarizations, their adsorbed hydrogen atoms bring the strongest repulsive interaction and then raise the potential energy of the critical system to a large extent. Thus, we have a large decrease in the reaction rate. The (1 1 0) and (1 0 0) planes do not have such sites.

(4) The experimental data, however, did not show such a unique behavior. It will be due to the method used, i.e. galvanostatic method where pulses of constant currents were imposed to electrode. At high polarizations, a fraction of the imposed current must be used for the hydrogen evolution and the rest must be for other reactions such as sodium ion discharge. The above theoretical prediction should be examined by a potentiostatic method.

(5) The theoretical predictions about the difference among the crystal planes are the subject to be examined in the future by using atomically identified planes. At the time of calculation, Ni single crystal electrode was not available.

5. Hydrogen evolution reaction on Pt single crystal electrode

In 1980, a new era opened for the study on a single crystal electrode. Clavilier et al. [22] reported a pioneering work on a Pt single crystal electrode prepared in their laboratory. A cyclic potential sweep at the electrode revealed a very interesting current-potential profile called 'voltammogram' which has attracted all the electrochemists in the world. Their method of preparing single crystal is practical in laboratories indeed and encouraged so many electrochemists. Nowadays, electrodes of noble metals exposing any crystal planes desired have become available in laboratories.

Thus, it is really a chance to ask how each crystal plane will behave toward the hydrogen evolution reaction. In our laboratory, a semi-spherical Pt single crystal electrode (dia: ca. 3 mm) with a flat crystal plane of interest was used. The plane was kept in contact with electrolyte solution (0.5 M H_2SO_4 saturated with inert gas) through meniscus (Fig. 5 inset). When required, the electrode was rotated keeping the meniscus.

5.1. Voltammograms

Let us first introduce the voltammograms on Pt low index planes, though they are well known to electrochemists, to understand how they are structure-sensitive (Fig. 5).

When electrode potential is swept in the positive direction from 60 mV, a positive current flows due to an oxidation of adsorbed hydrogen atoms and ceases at ca. 450 mV on the (1 1 1) plane. On the way back a negative current starts flowing from the same potential of ca. 450 mV due to the formation of the adsorbed hydrogen atoms from proton and draws a profile exactly symmetrical to the one observed on the positive going potential sweep. This current-potential profile is called 'hydrogen wave'. The adsorbed hydrogen atom of the wave is called Upd-hydrogen (Upd-H) since it deposits under (at more positive than) the equilibrium potential of the hydrogen electrode.

The above symmetrical feature of the hydrogen wave reflects a reversible nature of the Upd-H ionization and formation steps. The wave area also gives us an important information how many Upd-H we have on the surface. The hydrogen wave of Pt(1 1 1) plane gives a value almost equivalent to a monolayer value estimated from a geometrical area of the electrode, reflecting a full coverage of the surface with Upd-H at 60 mV. This indicates that the hydrogen evolution takes place on the surface covered fully with Upd-H when the electrode is polarized more negative than 60 mV in the solution saturated with an inert gas. A spike at ca. 450 mV has been discussed with a specific adsorption of anion, HSO_4^-.

The hydrogen wave changes its shape systematically with indexes of the surface. Fig. 5 shows typical waves on the other two low index planes. The waves are very structure-sensitive. A bell-shaped wave of the (1 1 0) plane locates least positive, indicating that Upd-H is least stable.

Voltammogram is a good example which shows a great advantage of an electrochemical approach that can tell us directly monolayer informations about adsorbed species as well as reacting species on a tiny but well defined surface. A carefully prepared electrolyte solution allows the surface clean, free from impurities for a considerable duration.

Common to the three index planes is that the electrode surface is fully covered with Upd-H at potentials less positive than 60 mV where the hydrogen evolution takes place.

5.2. Hydrogen evolution reaction

Hydrogen evolution was examined [23] by changing electrode potential in the negative direction from 60 mV in a step wise manner in order to obtain a steady current. At each polarization, a steady state was established within a few tens of seconds. The step duration was chosen as 2 min. To examine effects of evolved gas, if any, measurements were supplemented by rotating the electrode. A model reaction of ferrocyanide oxidation (2 mM $K_3[Fe(CN)_6]$ + 2 mM $K_4[Fe(CN)_6]$ + 0.5 M KCl) obeyed a linear Levich relation up to 10,000 rpm, showing the entire diffusion control. In the case of the hydrogen evolution reaction, the current stays almost constant, only 5–10% increase which was much less than expected from the decrease in diffusion layer thickness. The effect of the evolved gas was taken negligible and the electrode was kept static during the measurements. The Tafel plots on Pt(1 1 1), (1 0 0) and (1 1 0) planes are shown in Fig. 6.

Each plane confirms the Tafel relation of Eq. (13) in a potential range from 50 to −40 mV. The Tafel slope and $\log i_0$ on the respective planes are tabulated as follows.

Plane	(1 1 1)	(1 0 0)	(1 1 0)
Tafel slope (mV)	34	35	32
$\log\ i_0$ (mA cm^{-2})	−2.99	−2.97	−2.87

To our surprise, the same straight line appears independent of the crystal planes studied. This result is entirely different from what we predicted from the theoretical analysis on Ni electrode concluding that the reaction is highly structure-sensitive, i.e. Ni(1 1 1) plane is most active, the other planes are much less

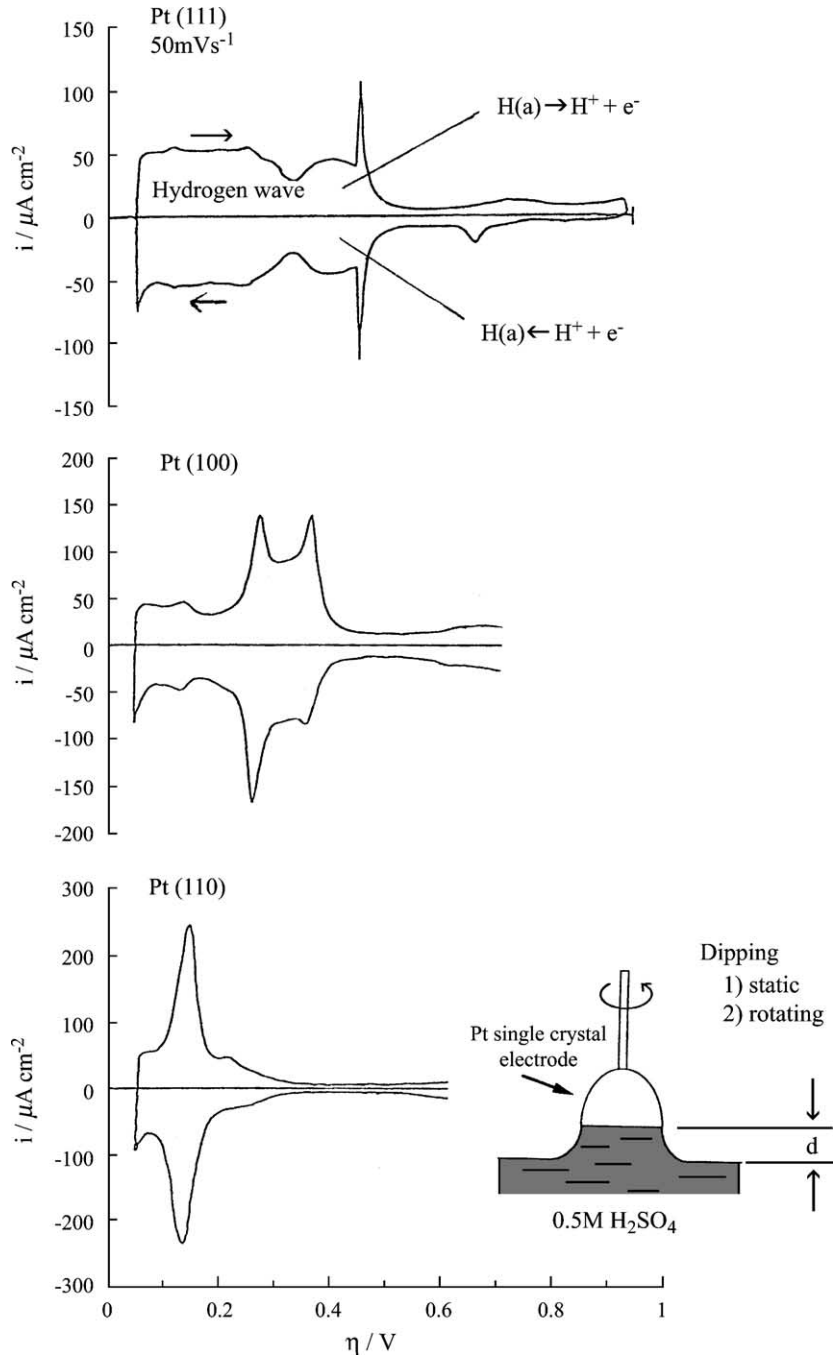

Fig. 5. Voltammograms on Pt(1 1 1), (1 0 0) and (1 1 0) planes in 0.5 M H_2SO_4 saturated with inert gas. Cyclic potential sweep (rate; 50 mV s^{-1}) was applied in a potential range from 60 mV to 1.0 V. Inset shows a semi-spherical Pt single crystal electrode at measurements.

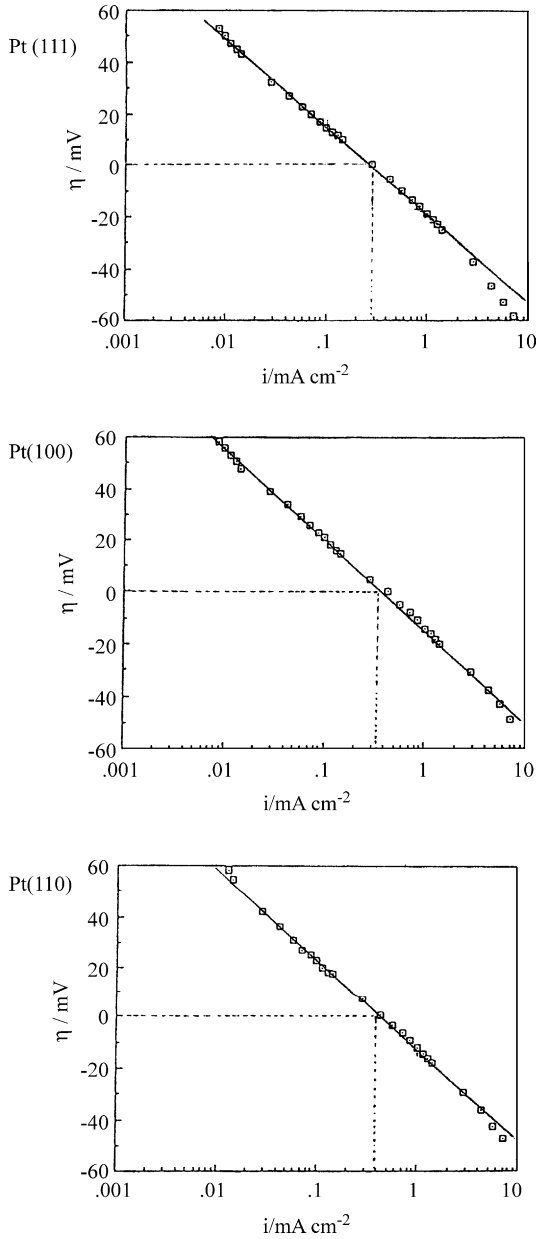

Fig. 6. Tafel plots of hydrogen evolution reaction on Pt(1 1 1), (1 0 0) and (1 1 0) planes in 0.5 M H_2SO_4 saturated with inert gas.

active and difference of their activities is larger than several orders of magnitude. This was not the case at the Pt single crystal electrodes.

Another aspect hardly accepted is the value of the Tafel slope. As discussed in the earlier section, the Tafel slope of 30 mV ($\alpha = 2$) is only acceptable for a surface being sparsely covered with H(a). However, the voltammograms clearly show that all the three low index planes are fully covered with Upd-H. Thus, the value of 30 mV strongly suggests the presence of another species being common among the planes studied and responsible for the hydrogen evolution. Toya [24,25] mentioned from quantum mechanical analysis that there exist two types of adsorbed hydrogen atoms on metals, named r- and s-type, respectively. The r-type is the hydrogen atom adsorbed on metal surface and s-type is the one solved in the surface.

A few years in advance of our measurements, Nichols and Bewick [26] reported a key information from their in situ IR spectroscopy observation that a new type of absorption band at 2090 cm^{-1} due to a hydrogen atom adsorbed on top of a surface Pt atom (on-top H, corresponding to the r-type) grows with a polarization more negative than about 80 mV on polycrystalline Pt and the Pt(1 1 1) plane in 1 M H_2SO_4. They concluded from correlations between the potential dependence of the band intensity and the rate of the hydrogen evolution that this on-top H is the reaction intermediate.

On-top site can be common among different Pt crystal planes and its structure-sensitive nature will be weakened to a large extent in comparison to those characteristic of the respective crystal planes such as three-fold sites in the (1 1 1) plane (corresponding to the s-type). Participation of on-top H as a real reaction intermediate is in good harmony with our Tafel relations observed as independent of the surface structure. In addition, the value of the Tafel slope, 30 mV, indicates a sparse population of on-top H in a potential range where the Tafel line is observed.

On the contrary, Upd-H's being present in a structure-sensitive manner to a full coverage do not participate in the hydrogen evolution. They are present just as the spectators. One should say that the art of nature is always so much instructive.

6. Conclusive comments

The hydrogen electrode reaction is one of the simplest reactions and has been studied by so many workers over a century of years. This is the only reaction which has been observed on all the metals except the

ones reactive with water. Thus, it is the best model reaction to search catalytic action of metals.

A pile of data accumulated so far tell that the catalytic activity expressed by i_0 (unidirectional rate at equilibrium) tremendously differs from metal to metal, e.g. more than 10^{10} times difference between Pt and Hg. To be mentioned is that when $\log i_0$ is plotted against atomic number of metals one can find a beautiful periodicity [27,28] common among three long periods of the periodic table. Such a periodicity suggests an important role of electronic structure of metals in determination of their catalytic activities. Details are the question to be solved in the future.

Nowadays, not only the single crystal electrodes with crystal planes identified to an atomic level but also a number of sophisticated instruments have come into wide use in electrochemical system under purified conditions.

Such a promising movements in electrochemistry will undoubtedly bring Horiuti's treatment the time to be highly appreciated with further advanced developments under much more precise informations on the reaction circumstances.

References

[1] J. Horiuti, M. Polanyi, Acta Physicochim. USSR 2 (1935) 505.
[2] J. Horiuti, M. Polanyi, Nature 132 (1933) 819.
[3] J. Horiuti, M. Ikushima, Proc. Imp. Acad. Jpn. 15 (1939) 39.
[4] J. Horiuti, Bull. Chem. Soc. Jpn. 13 (1938) 210.
[5] J. Horiuti, J. Res. Inst. Catal., Hokkaido Univ. 1 (1948–1951) 8.
[6] J. Tafel, Z. Physik. Chem. 50 (1905) 641, 713.
[7] J. Brönsted, K. Pedersen, Z. Physik. Chem. A108 (1924) 185.
[8] J. Horiuti, G. Okamoto, Sci. Pap. Inst. Phys. Chem. Res. (Tokyo) 28 (1936) 231.
[9] K. Hirota, J. Horiuti, Sci. Pap. Inst. Phys. Chem. Res. (Tokyo) 30 (1936) 151.
[10] K. Bonhoeffer, Z. Physik. Chem. 113 (1924) 199.
[11] J. Horiuti, H. Kita, J. Res. Inst. Catal., Hokkaido Univ. 12 (1965) 122.
[12] G. Okamoto, J. Horiuti, K. Hirota, Sci. Pap. Inst. Phys. Chem. Res. (Tokyo) 29 (1936) 223.
[13] J. Horiuti, J. Res. Inst. Catal., Hokkaido Univ. 4 (1956–1957) 55.
[14] T. Kwan, J. Res. Inst. Catal., Hokkaido Univ. 1 (1948–1951) 81.
[15] T. Kwan, Adv. Catal. 6 (1954) 67.
[16] J. Horiuti, K. Hirota, J. Res. Inst. Catal., Hokkaido Univ. 8 (1960) 51.
[17] H.A. Bethe, Proc. R. Soc. (London) A150 (1935) 552.
[18] R.E. Peierls, Proc. Cambridge Philos. Soc. 32 (1936) 471.
[19] J. Horiuti, T. Toya, J. Res. Inst. Catal., Hokkaido Univ. 12 (1964) 76.
[20] J. Horiuti, J. Res. Inst. Catal., Hokkaido Univ. 11 (1963) 55.
[21] H. Kita, T. Yamazaki, J. Res. Inst. Catal., Hokkaido Univ. 11 (1963) 10.
[22] J. Clavilier, R. Faure, G. Guinet, R. Durand, J. Electroanal. Chem. 107 (1980) 205.
[23] H. Kita, S. Ye, Y. Gao, J. Electroanal. Chem. 334 (1992) 351.
[24] T. Toya, J. Res. Inst. Catal., Hokkaido Univ. 6 (1958) 76.
[25] T. Toya, J. Res. Inst. Catal., Hokkaido Univ. 8 (1960) 209.
[26] J. Nichols, A. Bewick, J. Electroanal. Chem. 243 (1988) 445.
[27] H. Kita, Encyclopedia of electrochemistry of the elements, in: Hydrogen; Kinetics and Electrocatalysis, vol. IXa-3, Marcel Dekker, New York, 1982, p. 413.
[28] H. Kita, J. Electrochem. Soc. 113 (1966) 1095.